REGULARISED FEATURE-BASED FUZZY CONNECTEDNESS SEGMENTATION OF ULTRASOUND IMAGES FOR FETAL SOFT TISSUE QUANTIFICATION ACROSS GESTATION

Sylvia Rueda[1]*, Caroline Knight* [2]*, Aris T. Papageorghiou*[2]*, J. Alison Noble*[1]

[1] Institute of Biomedical Engineering, Department of Engineering Science, University of Oxford, U.K.
sylvia.rueda@eng.ox.ac.uk, noble@robots.ox.ac.uk
[2] Nuffield Department of Obstetrics & Gynaecology, University of Oxford, U.K.
caroline.knight@obs-gyn.ox.ac.uk, aris.papageorghiou@obs-gyn.ox.ac.uk

ABSTRACT

Ultrasound (US) image segmentation can be a challenging task due to signal dropouts, missing boundaries, and presence of speckle. Typically, purely intensity-based methods do not lead to a good segmentation of the structures of interest. Prior work has shown that local phase and feature asymmetry, derived from the monogenic signal, extract structural information from US images. This paper proposes a novel US segmentation approach based on the fuzzy connectedness framework. The approach uses local phase and feature asymmetry to define the so-called affinity function, which drives the segmentation algorithm, incorporates a shape-based object completion step, and regularises the result by mean curvature flow. Identifying new image-based biomarkers of fetal nutrition across gestation is essential to characterise the well-being of a fetus at an early stage. Results are presented on US images of the fetal arm taken at multiple gestational ages, the adipose tissue being an indicator of the fetal nutritional state.

***Index Terms*—** Image segmentation, ultrasound, fuzzy connectedness, local phase, feature asymmetry, monogenic signal, c-scale, soft tissue, fetal imaging, biomarkers.

1. INTRODUCTION

Ultrasound (US) imaging is extensively used in clinical practice due to its non-invasive nature, real time acquisition, and reduced cost compared to other imaging modalities. However, US images can be challenging to analyse due to potentially low signal-to-noise ratio, signal dropouts, artefacts, missing boundaries, attenuation, shadows, and presence of speckle. This makes US image segmentation one of the most difficult and challenging among medical imaging modalities.

In clinical practice, tissues and organs need to be delineated accurately to quantify the structures of interest. However, automatic segmentation is especially challenging in US images where the object boundaries appear fuzzy or lost. Several approaches are available at present for segmenting B-mode US images [1]. Among these, the use of local phase, derived from the monogenic signal [2], has proven useful for a variety of image analysis tasks including segmentation [3] and feature detection [4], since it extracts structural image information while being invariant to contrast.

Fuzzy connectedness (FC) segmentation [5] is a region-based approach that takes into account the gradation of intensity values within an object by defining the strength of local "hanging togetherness" of pixels within an image, taking into account their spatial relationship and their intensity similarities within the object of interest. Prior work [6] proved that applying intensity-based FC to US images did not produce good segmentation results. However, by incorporating into the framework feature information extracted from local phase instead of image intensities, the local phase-based FC framework became invariant to contrast and thus suitable for US segmentation [6].

This paper builds significantly on the early implementation [6] and introduces a complete and novel framework for US image segmentation. The new approach is illustrated on US images of the fetal arm. Our research interest is in identifying new image-based biomarkers of fetal nutrition. Fetal adipose tissue in the limbs has been shown to be representative of the fetal nutritional state [7], and its quantification could be a good indicator of fetal growth [8]. In Section 2, the concepts of local phase and feature asymmetry are introduced. Section 3 describes the feature-based fuzzy connectedness segmentation approach. Section 4 defines a novel method for completion and regularisation of the results. Qualitative and quantitative evaluations are presented in Section 5. Conclusions are given in Section 6.

2. LOCAL PHASE AND FEATURE ASYMMETRY

The monogenic signal [2] $I_M(x,y)$ of an image $I(x,y)$ generalizes the analytic signal to $2D$ (nD) as $I_M(x,y) = (I_b(x,y), h_1(x,y) \otimes I_b(x,y), h_2(x,y) \otimes I_b(x,y))$, where $I_b(x,y)$ results from convolving $I(x,y)$ by a bandpass filter $b(x,y)$, $\otimes$ denotes the convolution operation, and h_1 and h_2 are the convolution kernels of the Riesz transforms, which are defined as $h_1(x,y) = x/(2\pi(x^2+y^2)^{\frac{3}{2}})$ and $h_2(x,y) = y/(2\pi(x^2+y^2)^{\frac{3}{2}})$, respectively. The local phase $\varphi(x,y)$ of $I(x,y)$ is derived from $I_M(x,y)$ and expressed as

$$\varphi = arctan\left(\frac{I_b}{\sqrt{(h_1 \otimes I_b)^2 + (h_2 \otimes I_b)^2}}\right). \qquad (1)$$

The key choice to be made is in the selection of the bandpass filter $b(x,y)$. In the proposed method, a Gaussian derivative filter [9]

This research was supported by the Wellcome/EPSRC Centre of Excellence in Medical Engineering - Personalised Healthcare, WT 088877/Z/09/Z. Aris Papageorghiou is supported by the Oxford Partnership Comprehensive Biomedical Research Centre funded by the Department of Health NIHR Biomedical Research Centres funding scheme. Medical images provided by the University of Oxford. Special thanks to Prof. Udupa and Dr. Cifor.

with scale σ was selected. Edge features can be detected at points of local phase congruency [10], obtained from computing the local phase at multiple scales and combined using the *feature asymmetry FA* measure defined as

$$FA = \frac{1}{N} \sum_{s} \frac{\lfloor |\boldsymbol{odd}_s| - |even_s| - T_s \rfloor}{\sqrt{even_s^2 + \boldsymbol{odd}_s^2} + \varepsilon}, \quad (2)$$

where $even = I_b$, $\boldsymbol{odd} = (h_1 \otimes I_b,\ h_2 \otimes I_b)$, $\lfloor . \rfloor$ sets to zero the negative values, s represents the scale, N is the total number of scales, ε is a constant that avoids the division by zero (typically $\varepsilon = 0.01$), and T_s is an orientation independent threshold that controls the spurious responses to noise at scale s [4, 10]. *FA* is close to 1 near boundaries and close to 0 in homogeneous regions.

Thin edge map from Feature Asymmetry

The *FA* image consists of thick detected edges and a good localisation of the edges of the object of interest is essential in this framework. In a prior version [6], thinning, using mathematical morphology, was applied to the edges of the FA image. However, the resulting edges were not accurately localized. To overcome this, a modified non-maximal suppression technique was developed. First, for each pixel in the FA image, non-maximal suppression is computed in all possible directions. Then, at each pixel, the maximum value among all directions is retained. This strategy captures the relevant edge information with good localization while retaining the same intensity present in the FA image, thus obtaining the edge map *E* that will be used in this work.

3. FEATURE-BASED FUZZY CONNECTEDNESS

Fuzzy Connectedness [5] has proven to be effective (in terms of precision, accuracy and efficiency) in segmenting tissues in the presence of intensity gradation in MR and CT images. The strategy is based on a *global* fuzzy relation that assigns a strength of connectedness to every pair of pixels in an image to define objects via dynamic programming. The key step of this region-based approach relies in the definition of a *local* fuzzy relation μ_κ, called *affinity*, which defines the local "hanging togetherness" between any two adjacent pixels. If two pixels c and d are adjacent, the affinity depends on how homogeneous the region is and on how close the difference of intensity values at c and d is from the expected intensity value of the object of interest. The affinity is equal to 0 for non-adjacent pixels. The affinity values are used to define a *global* relation, called Fuzzy Connectedness, where the strength of connectedness between any two pixels is calculated as the largest of the strengths of all paths between c and d on the discrete image grid. Each path corresponds to a sequence of adjacent pixels starting from c and finishing in d and has a corresponding strength value, which is the smallest affinity of any pair of consecutive pixels along the path (weakest link). The fuzzy connectedness is represented as a connectivity map, where the object of interest is obtained by thresholding the image at T_{FC}. The initialisation of the method is based on manually placing one or several seeds within the object of interest. A minimal training stage is required to define the mean and standard deviation of the object of interest.

The FC framework was adapted to US segmentation by defining a new affinity function that uses structural and edge feature information instead of intensities [6]. The affinity function was designed as follows. Assume that every fuzzy subset $\mathcal{A}$ in a set is characterised by its membership function $\mu_{\mathcal{A}}$ with values in $[0, 1]$. Given an image, the affinity is composed of three factors: an adjacency component μ_α, an object feature-based component μ_ϕ, and a homogeneity-based component μ_ψ. The adjacency component μ_α is a non-increasing function of the distance $\|c - d\|$ defined as

$$\mu_\alpha(c, d) = \begin{cases} 1, & \text{if } c = d \text{ or } \|c - d\| = 1, \\ 0, & \text{otherwise.} \end{cases} \quad (3)$$

In the original framework [5], the object feature-based component was defined based on the intensities of the image, whereas the homogeneity-based component was a measure of intensity gradient. The proposed method incorporates the local phase information into the object-feature based component, extracting structural information and making the image invariant to contrast. The edge map E, derived from feature asymmetry, directly gives a measure of homogeneity, since smooth regions have small values and regions near boundaries have large values (cf. Sect. 2). Therefore, it is natural to consider it in the definition of the homogeneity-based component. Let $\varphi(c)$ and $E(c)$ be the local phase and thinned edge map derived from feature asymmetry at pixel c, respectively. The homogeneity-based component μ_ψ will have a high affinity in homogeneous regions and small affinity at the edges. Since *E* is close to 0 in homogeneous regions and close to 1 at the boundaries, we can express the homogeneity component as

$$\mu_\psi(c, d) = 1 - E(c). \quad (4)$$

The object feature-based component μ_ϕ takes into account characteristic features of the object of interest. In this paper, a recent formulation [11] was applied directly to the local phase image instead of intensities, as follows:

$$\mu_\phi(c, d) = e^{-\max\{\|\varphi(c) - m_o\|, \|\varphi(d) - m_o\|\}^2 / 2\sigma_o^2}, \quad (5)$$

where m_o and σ_o are the mean and standard deviation of the object of interest, previously calculated in a training stage.

There exist several ways of combining the affinity components to form the fuzzy affinity μ_κ [11]. One general form commonly used is $\mu_\kappa(c, d) = \mu_\alpha(c, d)[\omega_1 \mu_\phi(f(c), f(d)) + \omega_2 \mu_\psi(f(c), f(d))]$, where $f(c)$ and $f(d)$ correspond to the intensities at pixels c and d, respectively [5]. The equivalent affinity function for the present approach is expressed as

$$\mu_\kappa(c, d) = \mu_\alpha(c, d)[\omega_1 \mu_\phi(\varphi(c), \varphi(d)) + \omega_2 \mu_\psi(E(c))], \quad (6)$$

where $\omega_1 + \omega_2 = 1$, and with μ_ψ and μ_ϕ as defined in (4) and (5), respectively. The method was implemented in Matlab, using C mex files for faster computation.

4. DELINEATING CLOSED REGIONS AND REGULARISATION

The segmentation resulting from the feature-based FC only incorporates regions of the object of interest present in the image but is unable to delineate the information in shadowed areas (e.g. Fig.1(b)), as there is no ultrasonic signal response from this region. To overcome this, a novel object completion technique has been developed. This first detects the region of the object of interest occluded by a shadow, and then fills the gap in by using local shape constraints. The completion step works as follows.

First, the convex hull of the segmentation result is computed and its boundary extracted. For each boundary element, a local curvature-scale shape descriptor [12], called c-scale, is used to define the tangent at each point in the curve. The c-scale method has proven to be robust in obtaining a complete description of shape directly applied to digital boundaries. From the tangents, the normals to the convex hull contour are calculated at each boundary point in the direction pointing towards the inside of the object. Then, the binary intersection between each normal and the segmented object (resulting from FC) is retrieved and the width of the segmented object at each boundary element is calculated. The hole (gap) is detected by finding the region with zero width. The two normals on each side of the hole are then identified.

The second step consists of filling in the gap in the segmented object. A polygon is constructed by connecting the two detected normals on each side of the hole at the level of the convex hull boundary from one side, and the segmented object boundary from the other side. The corrected object is obtained from the binary union between the polygon and the segmented object.

The resulting object is finally smoothed using a mean curvature flow (MCF) [1] regularisation [14].

5. RESULTS

A qualitative and quantitative evaluation of the proposed approach was performed on 20 cross-sectional US images of the fetal arm, all from normal pregnancies, acquired from different fetuses between 21 and 38 weeks of gestation, the object of interest being the adipose tissue (Fig.1). Note the characteristic shadow appearing under the humerus bone (Fig.1(b)), which prevents the visualization of adipose tissue in that area. Furthermore, in fetal US images, the quality decreases with gestational age, creating strong artefacts that difficult the segmentation task at later gestations. The methodology presented in this paper is applicable across gestation.

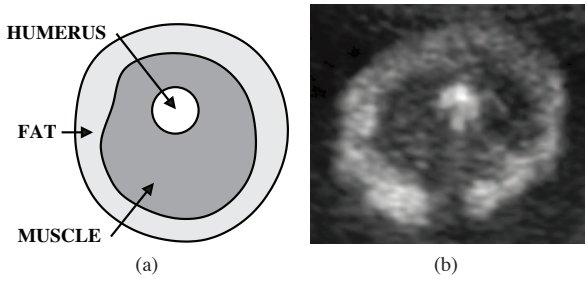


Fig. 1. (a) Schematic of arm composition. (b) Arm cross-section of a 27 weeks fetus with characteristic shadow under the humerus bone, due to lack of ultrasonic signal response from that region. Notice intensity inhomogeneities within the object of interest.

The method is automatic up to one to three clicks of initialisation. Fig.2 shows the main steps of the proposed methodology. The local phase image (Fig.2(a)) was obtained using a Gaussian derivative filter at scale $\sigma = 27$. The corresponding feature asymmetry (Fig.2(b)) was a result of combining three scales: $\sigma = 23$, $\sigma = 25$, and $\sigma = 27$, and setting $T_s = 0.155$, calculated from statistical properties of the local phase image. From the feature asymmetry image, the edge map to be used within the feature-based FC can be computed, as shown in Fig.2(c). Within the FC framework, the object feature-based component of affinity (5) obtains the mean $m_o = 2.44$ and the standard deviation $\sigma_o = 3 \times 0.086$ from a region of fat in the local phase image from a training stage. The images used for training were not part of the evaluation set. The final affinity (6) was calculated with $\omega_1 = \omega_2 = 0.5$. The initialization of the method is achieved by placing one or more seeds in the fat layer of the image. In the set of images used, most of the images required one seed and few required 2 or 3, if presenting disconnected pieces of fat. The object of interest was thresholded from the connectivity map by using $T_{FC} = 0.85$. The segmentation result is displayed in Fig.2(d). Notice the small indentations in the segmented object. These are due to the small "feather-like edge segments" appearing on the main edges of the edge map (Fig.2(c)). Pruning could have been used to remove the feathers and obtain a cleaner initial segmentation. However, our experiments indicate that the regularisation step takes care of this as well, and therefore this extra step is not required, as shown in Fig.2(e), where the object completion step was included.

Quantitative results are presented in Table 1, where the segmentation results (S) on 20 US images of the fetal arm are compared with the manual segmentations, considered as the reference method (RM), in terms of precision (P), recall (R), and Dice (D) similarity, defined as:

$$\mathrm{P} = \frac{|\mathrm{RM} \cap \mathrm{S}|}{|\mathrm{S}|},\ \mathrm{R} = \frac{|\mathrm{RM} \cap \mathrm{S}|}{|\mathrm{RM}|}, \text{and } \mathrm{D} = \frac{2|\mathrm{RM} \cap \mathrm{S}|}{|\mathrm{RM}| + |\mathrm{S}|}, \quad (7)$$

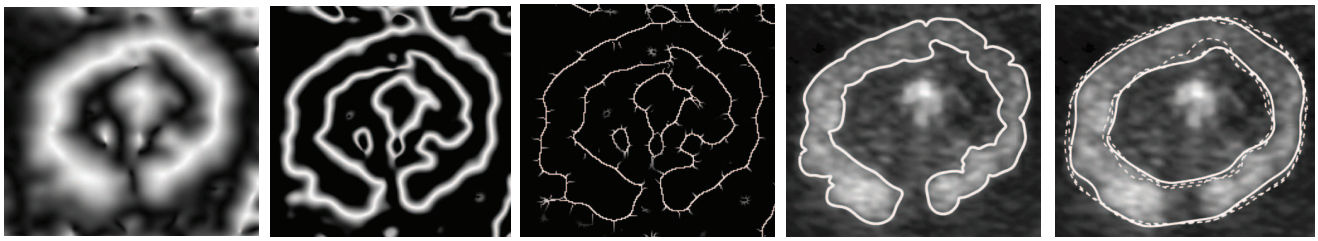
where $|.|$ refers to the number of elements in the set. Manual segmentations were performed by one clinician twice per image. Several variants of the method are compared to the reference method, including results using the earlier implementation (without the regularisation and object completion steps) [6]. The manual segmentations had an overall precision of $94.28 \pm 3.64\%$, a recall of $87.55 \pm 5.73\%$, and a Dice similarity of $90.01 \pm 2.71\%$, which are very close to the proposed method (referred in Table 1 as FC+C+MCF). The influence of the object completion and regularisation steps are analysed separately, showing that the performance of the feature-based FC with completion of the annular shape followed by the regularisation step is the best. The order in which the object completion and the regularisation steps are performed is important. Using the object completion after the regularisation step gives slightly worse results because small shape differences are incorporated into the overall object shape after object completion, and these need to be smoothed together with the rest of the object.

Table 1. Comparison of methods with manual segmentation. (FC: Feature-based FC - C: completion - MCF: regularisation)

Method	**Precision** (%)	**Recall** (%)	**Dice** (%)
FC [6]	87.91 ± 6.24	80.31 ± 5.03	83.57 ± 2.63
FC+MCF	90.30 ± 5.64	79.42 ± 4.93	84.17 ± 2.18
FC+C	89.08 ± 5.68	82.28 ± 4.65	85.25 ± 2.69
FC+MCF+C	89.83 ± 5.66	83.37 ± 4.63	86.17 ± 2.51
FC+C+MCF	88.75 ± 5.88	85.17 ± 4.56	86.62 ± 2.73

The automatic quantification of adipose tissue was obtained using the described methodology on 20 healthy fetuses, showing for the first time adipose tissue growth across gestation (Fig3).

[1] http://www.cs.ubc.ca/∼mitchell/ToolboxLS/ [13]



(a) Local Phase (b) Feature Asymmetry (c) Edge map (d) Feature-based FC only (e) Final Segmentation

Fig. 2. Main steps of the proposed method applied to Fig.1(b). (a) Local Phase at $\sigma = 27$. (b) Feature asymmetry with $\sigma = 23$, $\sigma = 25$, $\sigma = 27$. (c) Edge map extracted from feature asymmetry using non-maximal suppression in all directions. (d) Feature-based FC segmentation result. (e) Final segmentation obtained from feature-based FC after completion and regularisation. Both manual segmentations are displayed in dashed lines. Continuous lines show the proposed segmentation results.

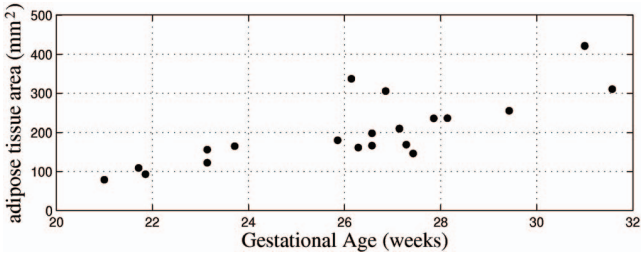


Fig. 3. Adipose tissue (mm^2) vs gestational age (weeks) measured with the proposed approach applied to 20 cross-sectional images of the fetal arm, representing normal growth.

6. CONCLUSIONS

This paper presents a complete automatic US image segmentation framework based on a feature-based FC segmentation method. The approach uses structural and edge information based on local phase, instead of intensities and intensity gradients, to drive the segmentation. The resulting segmentation is then completed by filling the gap caused by shadows in the segmented object of interest. A final regularisation based on mean curvature flow is performed. The quantitative and qualitative results were illustrated on 20 cross-sectional images of the fetal arm across gestation, showing a good performance with respect to manual segmentations. The amount of fetal adipose tissue across gestational ages for healthy fetuses was also presented for the first time, showing the growth trajectory of this indicator of fetal nutritional state. In future work, a comparison of these values with intra-uterine growth restricted fetuses will be conducted, to study if an early detection of this condition can be achieved by using this image-based biomarker, as this could affect neonatal outcome.

The proposed method is general in the sense that it can be adapted to segment other objects in other applications (e.g. cardiac images) making good use of the edge and structural features.

7. REFERENCES

[1] J. A. Noble and D. Boukerroui, "Ultrasound image segmentation: a survey," *IEEE Trans Med Imaging*, vol. 25, no. 8, pp. 987–1010, 2006.

[2] M. Felsberg and G. Sommer, "The monogenic signal," *IEEE Trans. Signal Process.*, vol. 49, no. 12, pp. 3136–3144, 2001.

[3] A. Belaid, D. Boukerroui, Y. Maingourd, and J.F. Lerallut, "Phase-based level set segmentation of ultrasound images," *IEEE Trans. Inf. Technol Biomed.*, vol. 15, no. 1, pp. 138–147, 2011.

[4] M. Mulet-Parada and J. A. Noble, "2d+t acoustic boundary detection in echocardiography," *Med Image Anal*, vol. 4, no. 1, pp. 21–30, 2000.

[5] J.K. Udupa and S. Samarasekera, "Fuzzy connectedness and object definition: Theory, algorithms, and applications in image segmentation," *CVGIP*, vol. 58, no. 3, pp. 246–261, 1996.

[6] S. Rueda, C. Knight, A.T. Papageorghiou, and J.A. Noble, "Local phase-based fuzzy connectedness segmentation of ultrasound images," *Proceedings of MIUA*, pp. 331–335, 2011.

[7] G. Larciprete, H. Valensise, B. Vasapollo, G.P. Novelli, E. Parretti, F. Altomare, G. DiPierro, S. Menghini, G. Barbati, G. Mello, and D. Arduini, "Fetal subcutaneous tissue thickness (sctt) in healthy and gestational diabetic pregnancies," *Ultrasound Obstet Gynecol*, vol. 22, pp. 591597, 2003.

[8] I.M. Bernstein, M.I. Goran, S.B. Amini, and P.M. Catalano, "Differential growth of fetal tissues during the second half of pregnancy," *Am J Obstet Gynecol*, vol. 176, pp. 2832, 1997.

[9] D. Boukerroui, J.A. Noble, and M. Brady, "On the choice of band-pass quadrature filters," *J. Math. Imaging Vis.*, vol. 21, pp. 53–80, 2004.

[10] P. Kovesi, "Image features from phase congruency," *Videre*, vol. 1, no. 3, 1999.

[11] K.C. Ciesielski and J.K. Udupa, "Affinity functions in fuzzy connectedness based image segmentation ii: Defining and recognizing truly novel affinities," *CVIU*, vol. 114, pp. 155–166, 2010.

[12] S. Rueda, J.K. Udupa, and L. Bai, "Local curvature scale: a new concept of shape description," *Proceedings of SPIE Medical Imaging: Image Processing*, vol. 6914, pp. 69144Q1–69144Q11, 2008.

[13] I.M. Mitchell, "The flexible, extensible and efficient toolbox of level set methods," *Journal of Scientific Computing*, vol. 35, no. 2-3, pp. 300–329, 2008.

[14] J.A. Sethian, *Level Set Methods and Fast Marching Methods*, 1999.